Journal of
Water & Climate Change

IWA PUBLISHING

Journal of Water and Climate Change Vol 13 No 3, 1462 doi: 10.2166/wcc.2022.258

Evaluating the impact of climate change on surface water resources in the upper Ganjiang River Basin, China

Peibing Song [a], Chao Wang [b,*], Gongbo Ding [c], Jiahui Sun [d], Lingzhong Kong [e,f], Mengtian Lu [a], Xiaohui Lei [b] and Hao Wang [a,b]

[a] College of Civil Engineering and Architecture, Zhejiang University, Hangzhou 310058, China
[b] State Key Laboratory of Simulation and Regulation of Water Cycle in River Basin, China Institute of Water Resources and Hydropower Research, Beijing 100038, China
[c] State Key Laboratory of Hydraulics and Mountain River Engineering, Sichuan University, Chengdu 610065, China
[d] School of Civil Engineering, Shandong University, Jinan 250061, China
[e] College of Hydraulic Science and Engineering, Yangzhou University, Yangzhou 225009, China
[f] College of Water Conservancy and Hydropower Engineering, Hohai University, Nanjing 210098, China
*Corresponding author. E-mail: wangchao@iwhr.com

PS, 0000-0002-2857-0086; LK, 0000-0002-9213-7463

ABSTRACT

Projecting surface runoff is a meaningful task for rational allocation and optimal scheduling of water resources. Aimed at exploring the impact of climate change on surface water resources, the basin-scale water-balance model coupled with the Budyko-type equation was developed for the upper Ganjiang River Basin (UGRB). Studies demonstrated that the Budyko-CY function is the optimal water-balance model, with a Nash–Sutcliffe efficiency (*NSE*) of 0.843 in the calibration period and 0.653 in the validation period, respectively. The increase in temperature by 1 °C may bring about a 2.5–4.7% runoff decline, while the 10% increase in precipitation may lead to a 12.1–14.3% runoff ascent. The annual mean temperature is expected to grow by 0.69, 0.68 and 0.97 °C in the next 30 years relative to that during the reference period, respectively. Similarly, the surface runoff is estimated to increase by 8.4, 6.5 and 5.0% on a multi-year average scale, respectively. This study is beneficial to provide possibilities for climate scenarios that may occur in the future, and the results presented herein are capable of giving a reference for the planning and management of water resources in the UGRB.

Key words: Budyko hypothesis, climate change, hydrological response, upper Ganjiang River Basin

HIGHLIGHTS

- The water-balance model based on the Budyko-type equation is applicable in the study area.
- The annual temperature is expected to rise by 0.69, 0.68 and 0.97 °C in the next 30 years under three climate scenarios.
- Multi-year mean runoff increases slightly with the variability of 8.4% (RCP2.6), 6.5% (RCP4.5) and 5.0% (RCP8.5).

1. INTRODUCTION

Based on the IPCC AR5, global annual mean temperature exceeded 0.85 °C since 1880, and the annual mean temperature in China increased >1.0 °C in the past three decades, which was dramatically higher than the world's average (Warszawski *et al.* 2014; Fang *et al.* 2018). In the next 30 years, surface temperature is expected to rise ranging from 2.4 to 6.1 °C in China, while annual runoff may increase roughly by 3–10% (Liu *et al.* 2014). Influenced by the monsoon climate, China has become particularly sensitive to the global warming, which may bring about a descent in streamflow in some basins, such as the lower Yellow River Basin (Piao *et al.* 2010). Research demonstrated that climate change was detected to be a dominant driving factor yielding runoff reduction in major basins across China, and it was estimated to account for 53.5% of streamflow changes during the period 2001–2014 (Liu *et al.* 2017). Furthermore, a change in climate owing to ascending temperature and intensified evaporation has aggravated the situation of hydrological cycles, altered spatio-temporal distribution of water resources and further enlarged the evolution of climatic variables (e.g., precipitation and evaporation), and these, in turn, will inevitably produce an effect on the ecological system (John *et al.* 2020). Therefore, projecting climate change

and its impacts on surface runoff are essential for allocation and scheduling of water resources, and researchers have conducted much significant work in recent years, basically following the pattern of future climate scenario design-hydrological model-impact assessment.

General circulation models (GCMs) have been used extensively to characterize future climate change, which can reflect the dynamic change of climate system through numerical simulation (Zinyengere *et al.* 2017). Employing the outputs provided by GCMs to drive a hydrological model is a widely adopted method in view of the fact that the hydrological model is a useful tool for simulating runoff processes (Chen *et al.* 2012). To compare the impact of two delta-change methods on different precipitation scenarios, Yuan *et al.* (2016) applied the Xinanjiang (XAJ) model to predict surface streamflow, and more accurate runoff estimates can be obtained in the watershed with stronger precipitation change signals in the Pearl River Basin. Zhu *et al.* (2019) used the Soil and Water Assessment Tool (SWAT) model to discuss the uncertainty of future runoff and concluded that monthly runoff increases are concentrated between May and October (July and August are not included) in the Biliu River Basin. Jin *et al.* (2020) employed the Variable Infiltration Capacity (VIC) model to depict the water cycle process, suggesting that annual precipitation may ascend while runoff may descend in the Yellow River source region. Yan *et al.* (2020) applied the Water and Energy Transfer processes in Large basins (WEP-L) model integrated with the global Bayesian model averaging (BMA) method to make the runoff projections become convincing and revealed that runoff in the Yellow River Basin during the period 2050–2070 would be extraordinarily lower than that in the baseline period. Although there are structural differences in different GCMs, the temperature changes they reflect are quite consistent, whereas precipitation features appear as large fluctuations across various models (Wen *et al.* 2016). Sun & Peng (2020) took the RCP4.5 scenario as an example to estimate the range of runoff variation and reported that future annual runoff varies between 268.9 and 544.2 mm from 2011 to 2100. In summary, the hydrological model makes it possible to obtain more potential changes and detailed information on various climatic characteristics of the catchment by predicting surface runoff and providing continuous simulations of daily and monthly runoffs. Moreover, this approach can enhance the simulation accuracy in surface runoff by making use of satellite-based data (Crow & Ryu 2009). Nevertheless, considering that the hydrological model is a data-intensive method, an estimation of future runoff is complicated and fraught with uncertainties. Also, this approach is always constrained by multiple data sets (e.g., vegetation, topography, soil) (Teng *et al.* 2012). Thus, it is evident that a variety of uncertainties are introduced through the hydrological model in the form of model parameters and structures, and the impact generated by the hydrological model may be unneglectable especially for the complex model (Thompson *et al.* 2013). As a consequence, the hydrological model may not be the most appropriate choice to estimate future runoff in some cases, and it may be inapplicable for the large-scale catchment with insufficient data or limited hydrological information.

In contrast with the hydrological model, the water-balance method is identified as an alternative technique owing to its fewer model parameters and simpler calculation principles, and this approach has received tremendous attention in speculating the hydrological process under changing environments. Chen *et al.* (2017) analyzed that >60% watersheds in China would face water deficiency and revealed the increasingly unbalanced distribution of water resources since the middle of the last century. Xing *et al.* (2018) established an elasticity method to estimate future runoff in 35 catchments across China, and the Wang–Tang equation was the most reasonable water-balance equation to strengthen the prediction reliability. Yuan *et al.* (2018b) constructed a basin-scale water-balance approach and investigated that natural runoff would increase by 14.4–16.8% under the RCP4.5 scenario over the Yellow River Basin. Zhang *et al.* (2018b) quantified the impact of leaf area index (LAI) changes on the streamflow, and it is estimated that the downtrend in runoff is likely to sustain. Li *et al.* (2020) applied the elasticity method coupled with the Blaney–Criddle equation into the upper Heihe River Basin and reported that the predicted runoff may decline by 5.6 and 6.7% during two periods 2021–2050 and 2051–2080, respectively. Guan *et al.* (2021) established the elasticity method to predict runoff and investigated that increasing runoff during the projection period may alleviate water shortages in northern China. Previous studies have illustrated the feasibility of the water-balance model coupled with GCMs in ascribing future streamflow patterns, and the estimated runoff calculated from the Budyko's framework is quite similar to that calculated from the hydrological model (Li *et al.* 2013). It is also worth pointing out that investigative assessments are always earlier than the hydrological modeling, where the Budyko hypothesis is widely accepted to address the trouble of flexibly distinguishing the influences of climate change on surface streamflow (Kazemi *et al.* 2019). Furthermore, the water-balance model based on the single-parameter Budyko-type equation is particularly suitable for ungauged catchments, because only estimates of long-term water availability are needed in these catchments (Chiew 2010).

The Ganjiang River Basin (GRB), located in southern China with abundant water resources, is the largest and longest river in Jiangxi province. Over the past decades, the GRB has undergone severe water shortages. The contradiction between water supply and demand is particularly remarkable, and the phenomenon of upstream and downstream competition for water resources is increasingly highlighted in the dry season (Zhang *et al.* 2018a). Multi-year mean runoff in the upper Ganjiang River basin (UGRB) accounts for about 22.5% of that in the Poyang Lake Basin (PLB), and it is the largest among all three-grade water resource partitions over the PLB (Yu *et al.* 2014). Projecting future surface runoff in the UGRB is crucial for minimizing these adverse impacts, as it would be beneficial to develop more effective adaptation measures and achieve sustainable water resource management. Aimed at probing into climate change and its effects on surface water resources in the UGRB, this study is organized as follows: (1) to calibrate a single parameter within the Budyko's framework and compare the feasibility of various water-balance models, and to seek for the optimal Budyko-type equation for capturing the runoff variation; (2) to build the statistical relation between temperature and potential evapotranspiration and to investigate the sensitivity of surface runoff to climatic variables; and (3) to further project the future changes of hydrometeorological factors during the period 2021–2050 under various GCMs, with taking multiple representative concentration pathways (RCPs) into account. The research framework of this paper is shown in Figure 1.

2. DATA AND METHODS

2.1. Study area

The GRB is situated in 113°34′–116°37′E and 24°31′–28°45′N, covering an area of >83,500 km^2. As the longest river of the PLB, the Ganjiang reaches a length of 766 km and lies mainly in the Jiangxi Province. The GRB has four distinctive seasons, that is, summers are hot and rainy while winters are dry and cold, with annual precipitation ranging from 1,400 to 1,800 mm and mean temperature of 17.8 °C (Song *et al.* 2020).

The Wan'an Reservoir is located 2 km upstream of Wan'an County, and it plays an important role in alleviating the water crisis and maintaining the availability of water resources. The Dongbei hydrological station is the outlet control station over the UGRB, which can well reflect the runoff changes of the study area. Annual rainfall amount, surface water resource amount, and groundwater resource amount in the UGRB are 633.2×10^8, 344.7×10^8 and 95.9×10^8 m^3, equivalent to 1,574, 857 and 238 mm, respectively (Yu *et al.* 2014). The location of the UGRB is illustrated in Figure 2.

2.2. Data

Monthly runoff data from 1959 to 2017 were supplied by the hydrological yearbook issued by the local hydrological bureau. Observed daily meteorological data (1959–2017) of 13 meteorological stations (i.e., Ganxian, Changting, Guangchang, Ji'an-xian, Xunwu, Longnan, Nanxiong, Ninghua, Ningdu, Nanfeng, Yongfeng, Suichuan and Jingangshan, labeled in Figure 2) were collected from the National Meteorological Information Centre (NMIC). The Penman–Monteith method is employed to calculate potential evapotranspiration for a single meteorological station. Daily precipitation, temperature and

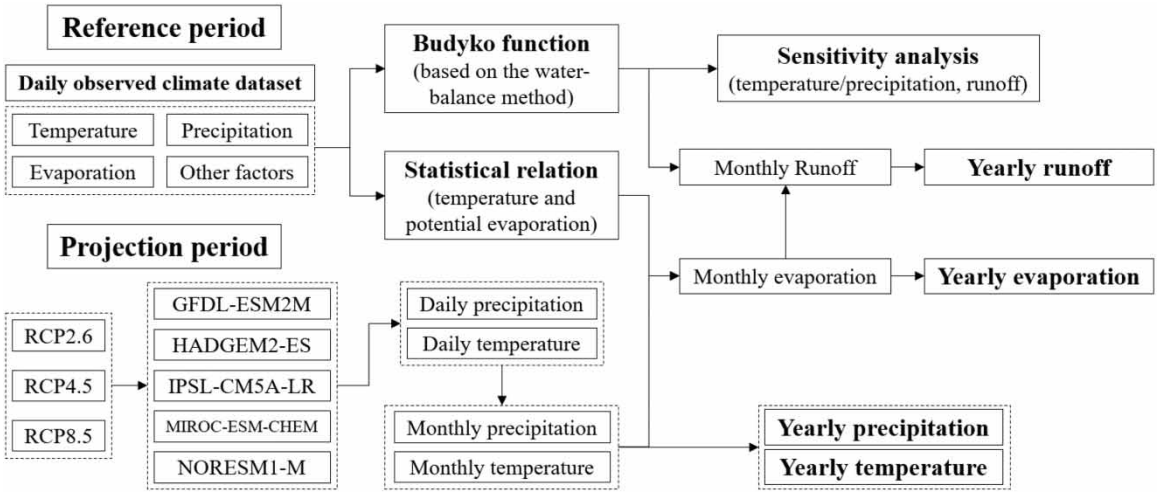

Figure 1 | Research framework of this paper.

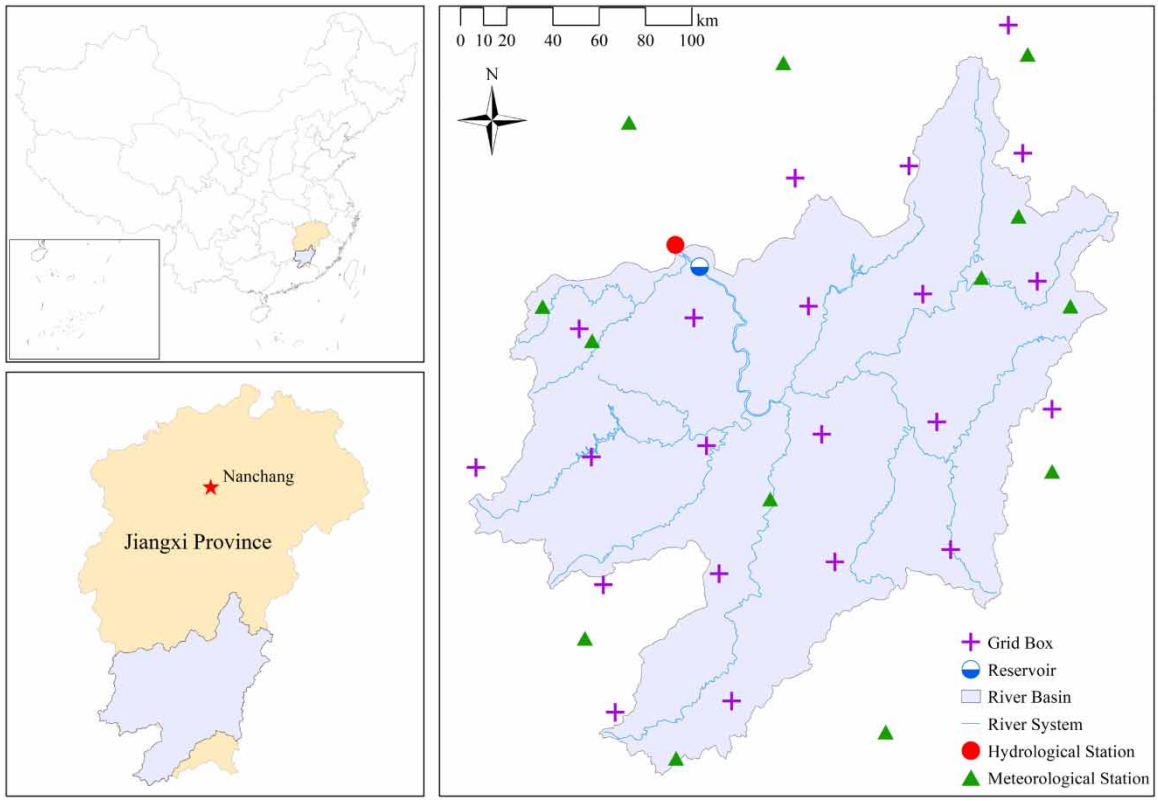

Figure 2 | Location of the UGRB.

evapotranspiration of the single station are reorganized into monthly precipitation, temperature and evapotranspiration, and then precipitation, temperature and evapotranspiration in the study area are calculated according to the Thiessen polygons method, respectively. It should be noticed that runoff depth is used to represent surface water resources. Precipitation, evapotranspiration and surface runoff during the reference period (1961–2010) are 1,560, 1,466 and 821 mm, respectively.

2.3. Climate scenarios

RCPs were defined in terms of a possible range of global radiation forcing value in 2100, and future mitigation emission scenarios are ranked as RCP2.6, RCP4.5, RCP6.0 and RCP8.5. Supposing that the forcing level will reach the highest point at ~3 W/m^2 before 2100, if this value drops to 2.6 W/m^2 by 2100, it stands for the RCP2.6 scenario; if this value stabilizes without overshoot pathways to 4.5 W/m^2 after 2100, it represents the RCP4.5 scenario; if this value stabilizes without overshoot pathways to 6.0 W/m^2 after 2100, it means the RCP6.0 scenario; if this value climbs rapidly to 8.5 W/m^2 by 2100, it symbolizes the RCP8.5 scenario (Yuan *et al.* 2018a).

Continuous daily-series meteorological data were derived from multiple GCMs. These climate models were chosen since they were widely accepted with persuasive feasibility in climate impact studies in China and can provide possible explanations concerning future climate which might make differences to some significant areas (Zhou *et al.* 2018). In addition, it should be noticed that Yuan *et al.* (2019) have demonstrated that these five climate models chosen in this paper are applicable in the similar catchment, the Fu River basin. Meteorological data contained the period from January 1951 to December 2050, with the geographical scope covering 70.25°–140.25°E and 15.25°–55.25°N (Piani *et al.* 2010). Precipitation and temperature data used in this study were bias-corrected and resampled, so as to ensure consistency between the observed data and the predicted data. In this paper, the statistical downscaling method and bilinear interpolation were used to uniformly interpolate the output data to a 0.5° × 0.5° grid, and these data were corrected based on the statistical deviation of probability distribution. A detailed description of five GCMs is listed in Table 1 (Taylor *et al.* 2012).

Three RCPs including RCP2.6 (low), RCP4.5 (medium) and RCP8.5 (high) scenarios were chosen to project the future precipitation, temperature and discharge variation, and 21 grid cells representing the future climatic variables in and around the UGRB are marked in Figure 2.

Table 1 | Five GCMs used in this study

Model name	Originating country	Resolution (atmosphere)	Resolution (ocean)
GFDL-ESM2M	United States, Geophysical Fluid Dynamics Laboratory (GFDL)	2.0° × 2.5°	0.9° × 1.0°
HadGEM2-ES	United Kingdom, Met Office Hadley Centre (MOHC)	1.3° × 1.9°	0.8° × 1.0°
IPSL-CM5A-LR	France, Institut Pierre Simon Laplace (IPSL)	1.9° × 3.8°	1.2° × 2.0°
MIROC-ESM-CHEM	Japan, Model for Interdisciplinary Research on Climate (MIROC)	2.8° × 2.8°	0.7° × 1.2°
NoRESM1-M	Norway, Norwegian Climate Centre (NCC)	1.9° × 2.5°	0.5° × 1.1°

2.4. Water-balance model

For a closed catchment, its hydrometeorological characteristics conform to the water-balance principle:

$$E = P - Q \tag{1}$$

where E, P and Q signify evapotranspiration (mm), precipitation (mm) and runoff (mm), respectively. E can be defined a function of aridity index (ϕ):

$$\frac{E}{P} = f(\phi) = f\left(\frac{E_0}{P}\right) \tag{2}$$

where E_0 denotes potential evapotranspiration, namely evaporation capacity, mm. Here, an empirical Budyko curve was attempted to quantitatively describe the relation among precipitation, evapotranspiration and evaporation capacity. In contrast with the non-parametric function, the single-parameter function has the advantage of enhancing the interpretation of climatic characteristics, as well as describing geographical characteristics (Wu *et al.* 2017). The Budyko-Fu function, with only a single parameter needing to be calibrated, is demonstrated to provide estimates of annual runoff similar to other models (Fu *et al.* 2007). Nevertheless, in view of the fact that existing studies always assign a single Budyko-type equation to quantify the response of runoff to climate change without giving convincing evidence, a variety of frequently used methods including Budyko-WT, Budyko-Zhang and Budyko-CY were presented to seek out the optimal equation in reproducing the runoff change (Wang & Tang 2014; Wu & Miao 2017). What these Budyko-type equations have in common is that they use fixed parameters instead of allowing them to vary with the catchment. As a result, data requirements can be reduced and this approach can be implemented automatically in other frameworks. Taking the Budyko-Fu function as an example, it describes the quantitative relation among precipitation, evapotranspiration and evaporation capacity as follows:

$$\frac{E}{E_0} = 1 + \frac{P}{E_0} - \left[1 + \left(\frac{P}{E_0}\right)^{\alpha}\right]^{1/\alpha} \tag{3}$$

Then, substituting Equation (1) into Equation (3), the above equation can be simplified into:

$$Q = E_0\left\{\left[1 + \left(\frac{P}{E_0}\right)^{\alpha}\right]^{1/\alpha} - 1\right\} \quad \text{(Budyko – Fu)} \tag{4}$$

Similarly, runoff can be described by other Budyko-type equations:

$$Q = \frac{P^2}{E_0 + \omega E_0^2/P + P} \quad \text{(Budyko – Zhang)} \tag{5}$$

$$Q = P - \frac{P + E_0 - \sqrt{P^2(1 + E_0/P)^{\partial} - 4\partial(2 - \partial)E_0 P}}{2\partial(2 - \partial)} \quad \text{(Budyko – WT)} \tag{6}$$

$$Q = P - \left[\left(\frac{1}{E_0}\right)^k + \left(\frac{1}{P}\right)^k\right]^{-k} \quad \text{(Budyko – CY)} \tag{7}$$

where α, ω, ∂ and k are dimensionless parameters and can be calibrated in a given time period.

Observed data during the period 1959–2017 were adopted to calibrate and verify the water-balance model, and the study period was divided into two parts: the calibration period (1959–1998) and the validation period (1999–2017). Then, a calibrated water-balance model was driven by climatic variables during the projection period (2021–2050) provided by the GCMs, and the relative variation characteristics of simulated runoff are used to characterize the trend of runoff.

2.5. Sensitivity analysis

The sensitivity of runoff to climate change is expressed as the proportional change of simulated runoff, and it can be obtained by comparing simulations driven by changes in precipitation or temperature, keeping other climatic variables unchanged simultaneously (Bao *et al.* 2012). In this case, the hypothetical scenario involving runoff to a climate change can be expressed as a function as follows:

$$\delta(\Delta T, \Delta P) = \frac{f(T + \Delta T, P + \Delta P) - f(T, P)}{f(T, P)} \times 100\% \tag{8}$$

where T denotes the mean temperature, °C; P denotes the precipitation, mm; ΔT denotes the hypothetical changes in mean temperature, °C; ΔP denotes the hypothetical changes in precipitation, mm; $\delta()$ represents the sensitivity function of runoff to climate change; $f()$ represents the relation function between runoff and the climate scenario.

2.6. Evaluation indices

Three indices, namely the relative error (*RE*), the Nash–Sutcliffe efficiency (*NSE*) and the deterministic coefficient (*DC*), were adopted to evaluate the performance of various Budyko-type equations:

$$RE = \left|\frac{Q_{sim,i} - Q_{obs,i}}{Q_{obs,i}}\right| \times 100\% \tag{9}$$

$$NSE = 1 - \frac{\sum_{i=1}^{n}(Q_{sim,i} - Q_{obs,i})^2}{\sum_{i=1}^{n}(Q_{obs,i} - \overline{Q_{obs}})^2} \tag{10}$$

$$DC = \frac{\left[\sum_{i=1}^{n}(Q_{sim,i} - \overline{Q_{sim}})(Q_{obs,i} - \overline{Q_{obs}})\right]^2}{\sum_{i=1}^{n}(Q_{sim,i} - \overline{Q_{sim}})^2 \sum_{i=1}^{n}(Q_{obs,i} - \overline{Q_{obs}})^2} \tag{11}$$

where $Q_{sim,i}$ is the ith simulated runoff, mm; $Q_{obs,i}$ is the ith observed runoff, mm; $\overline{Q_{sim}}$ is the average value of simulated runoff, mm; $\overline{Q_{obs}}$ is the average value of observed runoff, mm; n is the number of observed runoff series. The smaller *RE*, the larger *NSE* and the higher *DC* provides a better performance of the Budyko-type function. With reference to pre-existing studies, if $NSE > 0.5$, $DC > 0.6$ and $RE < 15\%$, it means that this approach is applicable in the catchment (Yuan *et al.* 2017).

3. RESULTS AND DISCUSSION

3.1. Runoff simulations by the water-balance model

For reasons of ensuring the water-balance model performs well in the study period, it is most important to calibrate the parameters in various Budyko-type equations during the period 1959–1998, followed by verifying these parameters during the period 1999–2017. After calibration, dimensionless parameters α, ω, ∂ and k are 1.70, 0.03, 0.02 and 0.99, respectively. The performance for different Budyko-type equations is shown in Table 2.

It can be concluded that all *RE* are <11%, all *NSE* are >0.84 and all *DC* are >0.84 in the calibration period, while all *RE* are <15%, all *NSE* are >0.64 and all *DC* are >0.72 in the validation period. Therefore, it is evident that four Budyko-type equations are highly consistent in runoff simulation for meeting the requirements of accuracy, and the water-balance model is applicable in the study area.

In contrast with other equations, the Budyko-CY equation has a better performance with respect to the *NSE* during two periods. As a consequence, the Budyko-CY function was screened as the optimal equation to project the runoff variation in the near future (2021–2050). Comparison between the simulated runoff and the observed runoff is shown in Figure 3.

3.2. Sensitivity analysis of runoff to climatic factors

The statistical relation between monthly mean temperature and monthly potential evapotranspiration was established via the MATLAB toolbox, taking the observed data during the period 1961–2010 into account. Figure 4 shows that monthly temperature and evapotranspiration conform to the non-linear relation composed of an exponential function and a linear function, and it was clear that this equation can fit the statistical relation well with the square of correlation coefficient of 0.894.

Table 2 | Performance for different Budyko-type equations

Time	Indices	Budyko-Fu	Budyko-Zhang	Budyko-WT	Budyko-CY
Calibration period (1959–1998)	*RE*	11.0%	10.9%	10.9%	10.9%
	NSE	0.843	0.840	0.840	0.843
	DC	0.843	0.843	0.843	0.843
Validation period (1999–2017)	*RE*	14.5%	14.9%	14.8%	14.5%
	NSE	0.651	0.645	0.650	0.653
	DC	0.720	0.720	0.720	0.721

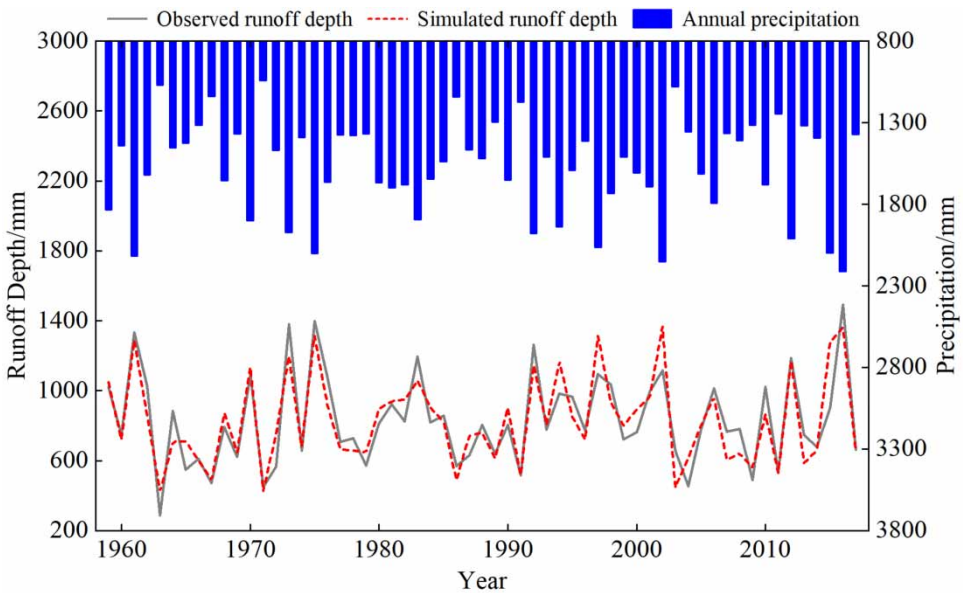

Figure 3 | Comparison between the simulated runoff and the observed runoff.

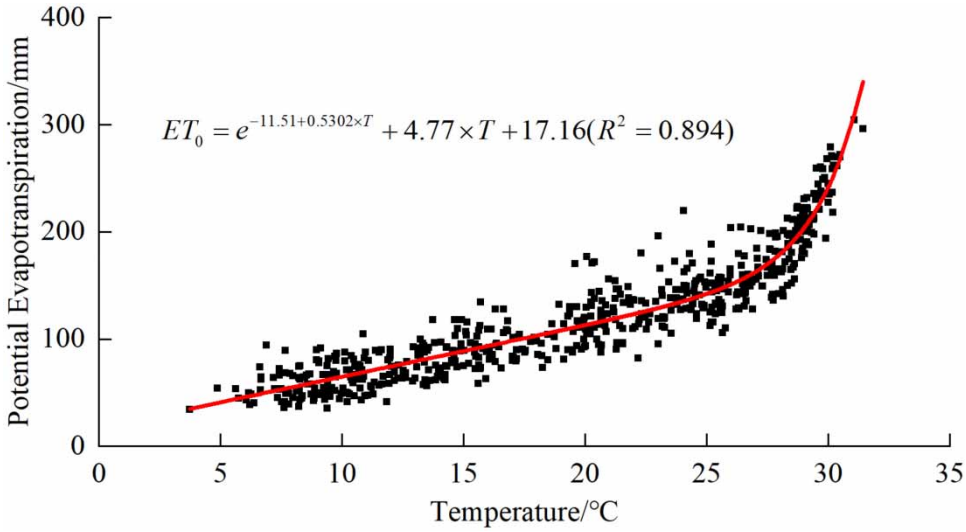

Figure 4 | Relations between monthly temperature and potential evapotranspiration.

Based on daily-series meteorological data of 21 grid cells in and around the UGRB generated by various GCMs, monthly precipitation and average temperature of 21 grid cells can be counted at first, and monthly precipitation and average temperature in the study area can be summarized. Then, monthly potential evapotranspiration in the study area can be calculated by means of the statistical relation proposed in Figure 4. Subsequently, surface runoff under multiple climate scenarios can be simulated with reference to the Budyko-CY function expressed in Equation (7). Ultimately, projected climate change and its possible influences on water resources can be estimated according to Equation (8), and the response of surface runoff to the variations in precipitation and temperature is shown in Figure 5.

In terms of the response of surface runoff to precipitation, on the condition of given precipitation, when annual temperature rises by 1 °C, the annual surface runoff is expected to decline by 2.5–4.7% on average, or 22.6–42.5 mm. In the case of a 30% ascent in precipitation, every 1 °C change in temperature may lead to the largest variation range in runoff, and corresponding runoff is expected to decrease by 7.8% when average temperature rises from 2 to 3 °C. Relatively speaking, in the case of a 30% reduction in precipitation, variation amplitude in runoff is the smallest for 1 °C change in temperature, and corresponding runoff is expected to decrease by 1.6% when average temperature changes from −3 to −2 °C. The foremost reason is that actual regional evaporation is relatively large under warm and humid conditions. Therefore, runoff is more sensitive to temperature rise under given precipitation.

In terms of the response of surface runoff to temperature, under the circumstance of given temperature, for every 10% increase in precipitation, annual surface runoff is expected to rise from 12.1 to 14.3% on average, that is, 110.7–130.6 mm. In the case of a 3 °C ascent in temperature, every 10% change in precipitation may cause the smallest variation range in runoff, and corresponding runoff is expected to increase by 11.0% when annual precipitation varies from −30 to −20%. Instead, in the case of a 3 °C reduction in temperature, variation amplitude in runoff is the largest for 10% variation in precipitation, and corresponding runoff is expected to increase by 15.0% when annual precipitation changes from 20 to 30%. Chiew (2010) revealed that the greater the runoff coefficient is in the watershed, the less sensitive it is to climate change. As far as the UGRB is concerned, its multi-year mean precipitation and streamflow during the period 1961–2010 are 1,560 and 821 mm, so the runoff coefficient is 0.53 over the UGRB. Therefore, the UGRB is not sensitive to climate change, and the analysis based on the water-balance model is consistent with it.

3.3. Future scenarios for hydrometeorological factors

3.3.1. Projected changes in monthly climatic factors

A comparison of three climatic factors is shown in Tables 3, where base represents the observed monthly average during the baseline period, while RCP2.6, RCP4.5 and RCP8.5 represent the projected ensemble mean value of five GCMs during the projection period (2021–2050).

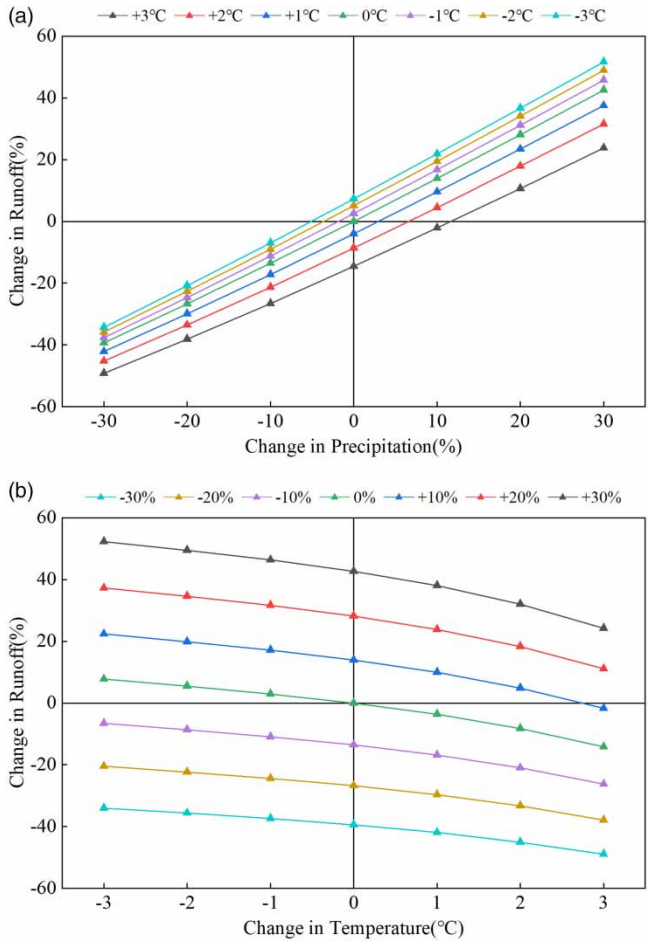

Figure 5 | (a) Response of surface runoff to the variation in precipitation and (b) the response of surface runoff to the variation in temperature.

In the next 30 years, the projected multi-year mean precipitation will vary as 10, −9 and −8 mm under three RCP scenarios, while the projected temperature will increase by 0.69, 0.68 and 0.97 °C, the projected potential evapotranspiration will increase by 162, 148 and 232 mm, respectively. Taking the temperature as an example, relative to the reference period, an average temperature will rise every month, especially in September and October, with warming by 1.1/1.1/1.6 °C and 1.0/0.9/1.2 °C under three RCPs. Similarly, the increased potential evaporation is mainly concentrated in July and August with monthly variation of 40/46/56 mm and 61/43/84 mm, respectively. The variation in monthly precipitation is specifically manifested as follows: rising in June, August and September, and falling in May, July and October.

3.3.2. Projected changes in annual precipitation

The projected annual precipitation in the UGRB is shown in Figure 6. The variation range and the ensemble mean for each RCP are shown concurrently, with the assumption that the ensemble mean is able to characterize the variation trend of annual precipitation, temperature and runoff, and five global climate models are equally plausible. It is worth noting that the solid lines in red, blue and green represent the multi-mode ensemble mean of annual runoff under three climate scenarios (i.e., RCP2.6, RCP4.5 and RCP8.5), respectively, whereas the dotted lines of corresponding colors represent the maximum and minimum annual runoffs in various GCMs during the projection period of 2021–2050. It is obvious that the annual precipitation under the RCP2.6 scenario presents the greater fluctuation of 558 mm due to its variation range, while that under both the RCP4.5 and RCP8.5 scenarios is 494 mm. The maximum and the minimum annual precipitation during the period of 2021–2050 are 2,465 mm (GFDL-ESM2M) and 900 mm (GFDL-ESM2M) under the RCP2.6 scenario, while they are 2,809 mm (GFDL-ESM2M) and 667 mm (MIROC-ESM-CHEM) under the RCP4.5 scenario and 2,560 mm (GFDL-ESM2M)

Table 3 | Comparison of (a) precipitation (mm), (b) temperature (°C) and (c) potential evapotranspiration (mm) between two periods

	Jan.	Feb.	Mar.	Apr.	May	Jun.	Jul.	Aug.	Sep.	Oct.	Nov.	Dec.	Sum
(a) Precipitation													
Base	64	100	171	208	241	244	131	141	94	69	54	43	1,560
RCP2.6	53	97	175	206	238	251	127	162	108	54	52	47	1,570
RCP4.5	61	98	164	211	231	244	129	151	101	60	58	43	1,551
RCP8.5	60	91	167	206	237	266	120	147	112	53	47	46	1,552
	Jan.	**Feb.**	**Mar.**	**Apr.**	**May**	**Jun.**	**Jul.**	**Aug.**	**Sep.**	**Oct.**	**Nov.**	**Dec.**	**Mean**
(b) Temperature													
Base	8.4	10.2	14.1	19.7	24	26.8	29.4	28.9	25.9	21.2	15.6	10.4	19.55
RCP2.6	8.8	10.6	14.7	20.1	24.6	27.6	29.9	29.7	27	22.2	16.4	11.3	20.24
RCP4.5	8.8	10.5	14.8	20.3	24.9	27.6	30	29.5	27	22.1	16.3	11	20.23
RCP8.5	9.1	10.7	14.9	20.7	24.8	27.9	30.3	30.1	27.5	22.4	16.6	11.2	20.52
	Jan.	**Feb.**	**Mar.**	**Apr.**	**May**	**Jun.**	**Jul.**	**Aug.**	**Sep.**	**Oct.**	**Nov.**	**Dec.**	**Sum**
(c) Potential evapotranspiration													
Base	60	60	79	108	139	151	226	195	155	131	91	71	1,466
RCP2.6	59	68	87	114	140	179	266	256	167	125	96	71	1,628
RCP4.5	59	67	88	114	142	176	272	238	169	124	95	70	1,614
RCP8.5	61	68	88	117	143	187	282	279	179	126	97	71	1,698

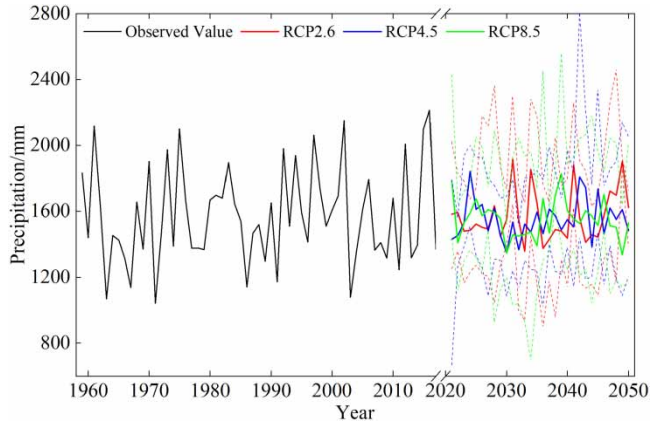

Figure 6 | Annual precipitation in the study area from 1959 to 2050.

and 693 mm (GFDL-ESM2M) under the RCP8.5 scenario, respectively. It is not difficult to find that the GFDL-ESM2M model is closely associated with annual rainfall extremes.

Figure 7 shows multi-year mean precipitation of various GCMs under three climate scenarios. It can be concluded that multi-year mean precipitation during the projection period changes by −8.5 to 8.7% (RCP2.6), −4.5 to 3.9% (RCP4.5) and −8.1 to 6.3% (RCP8.5), respectively. The average precipitation in the GFDL-ESM2M, HadGEM2-ES and NorESM1-M models will increase, with variation ranges of 1.6–7.2, 0.3–2.2 and 1.4–8.7%, while that in IPSL-CM5A-LR and MIROC-ESM-CHEM models will decrease, with variation ranges of −8.5 to −4.5% and −8.1 to −4.2%, respectively. In aggregate, the IPSL-CM5A-LR model has the minimum variation in future projected precipitation, with the average change of −6.9%, while the NorESM1-M model has the maximum variation with the average change of 5.4%.

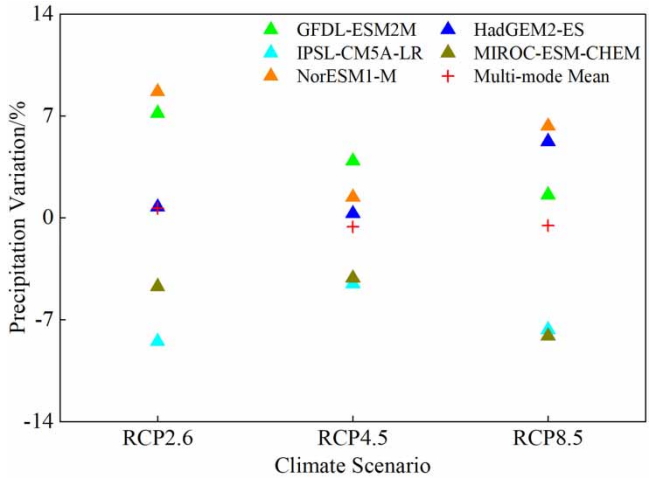

Figure 7 | Precipitation variation under various climate scenarios.

3.3.3. Projected changes in annual temperature

The projected annual temperature in the UGRB is shown in Figure 8. On a multi-year average scale, it is clear that temperature shows an upward trend in the projection period with the gradient of 0.29 °C/10a, 0.25 °C/10a and 0.61 °C/10a under three RCP scenarios, respectively. Especially in the last 10 years of the projection period, temperature is expected to increase by 1.03, 0.94 and 1.68 °C relative to that during the period of 1961–2010, suggesting that future temperature is expected to increase in the UGRB. The annual mean temperature under the RCP8.5 scenario presents the greater variation amplitude, with the maximum value of 21.74 °C in 2050 and the minimum value of 19.40 °C in 2040, while the variation amplitudes under RCP2.6 and RCP4.5 scenarios are 1.37 and 1.45 °C, revealing that the higher the temperature rises, the greater the variation range in temperature will be.

Figure 9 shows a multi-year mean temperature of various GCMs under three climate scenarios. From the perspective of RCP, the multi-year average temperature is expected to increase by 0.17–1.43 °C (RCP2.6), 0.22–1.18 °C (RCP4.5) and 0.53–1.72 °C (RCP8.5), respectively. When it comes to the GCM, all five models show a rise in temperature, with variation ranges of 0.22–0.53 °C (GFDL-ESM2M), 0.92–1.23 °C (HadGEM2-ES), 0.64–1.03 °C (IPSL-CM5A-LR), 1.18–1.72 °C (MIROC-ESM-CHEM) and 0.17–0.64 °C (NorESM1-M), respectively. The GFDL-ESM2M model has the minimum warming mean temperature of 0.33 °C, while the MIROC-ESM-CHEM model has the maximum warming mean temperature, reaching up to 1.44 °C under three RCPs. Different from the MIROC-ESM-CHEM and HadGEM2-ES models, the GFDL-ESM2M and NorESM1-M models both show a small increase in temperature under all RCP scenarios.

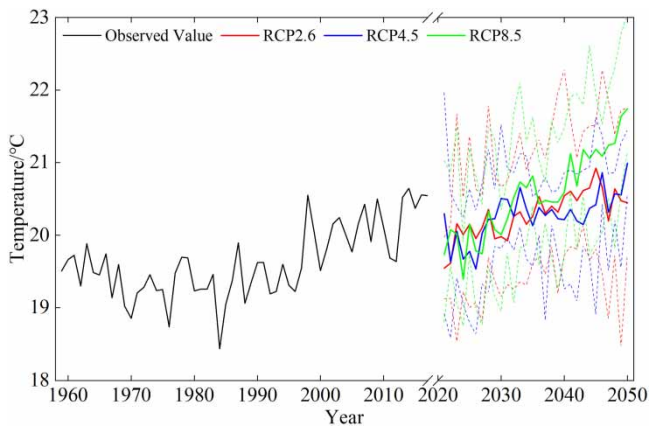

Figure 8 | Annual temperature in the study area from 1959 to 2050.

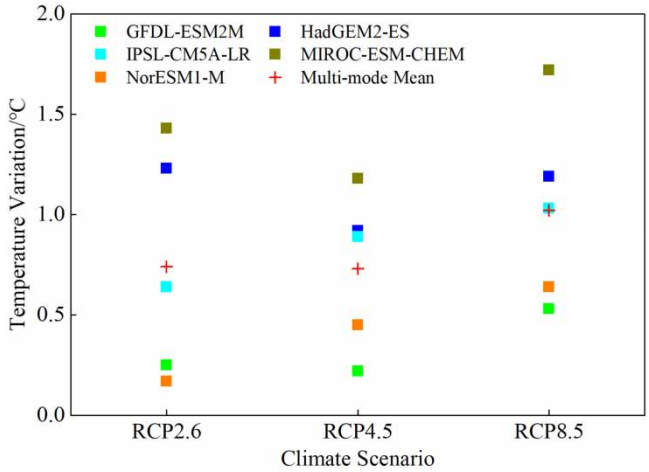

Figure 9 | Temperature variation under various climate scenarios.

3.3.4. Projected changes in annual runoff

The projected annual runoff in the UGRB is shown in Figure 10. The annual mean runoff is expected to increase by 8.4, 6.5 and 5.0% from 2021 to 2050 in contrast with that from 1961 to 2010, suggesting that surface water resources will increase in the next 30 years. The maximum runoff depth values are 1,190, 1,116 and 1,092 mm, while the minimum runoff depth values are 725, 692 and 662 mm under three RCPs, respectively. Studies demonstrated that a higher temperature may bring about a decrease in annual runoff in the UGRB. Nevertheless, different from RCP2.6 and RCP4.5 scenarios, the annual runoff under the RCP8.5 scenario shows a downward trend during the projection period, especially after 2040.

Figure 11 shows multi-year mean runoff depth of various GCMs under three climate scenarios. Surface water resources will increase in the future under various scenarios, except for the MIROC-ESM-CHEM model under three RCPs, as well as the IPSL-CM5A-LR model under RCP2.6 and RCP8.5 scenarios. The variation in projected runoff is similar between the GFDL-ESM2M model and the NorESM1-M model, because the former has the 21.2% ascent under the RCP2.6 scenario and 16.4% ascent under three RCPs, while those in the latter are 23.3% rise and 17.3% rise, respectively. On the contrary, the MIROC-ESM-CHEM model seems to be on a downward trajectory, with the variation amplitude of −12.5 to −2.1% and the mean variation value of −6.4%. The variation range under the RCP4.5 scenario is the smallest, varying from −2.05 to 16.02%, while variation ranges under RCP2.6 and RCP8.5 scenarios are −4.55 to 23.25% and −12.46 to 17.53%, respectively.

3.3.5. Discussions

The variations of the projected multi-year mean precipitation and temperature over the UGRB during the period 2021–2050 are relatively close to the conclusions proposed by Deng & Wang (2019), and both are precipitation declines and potential

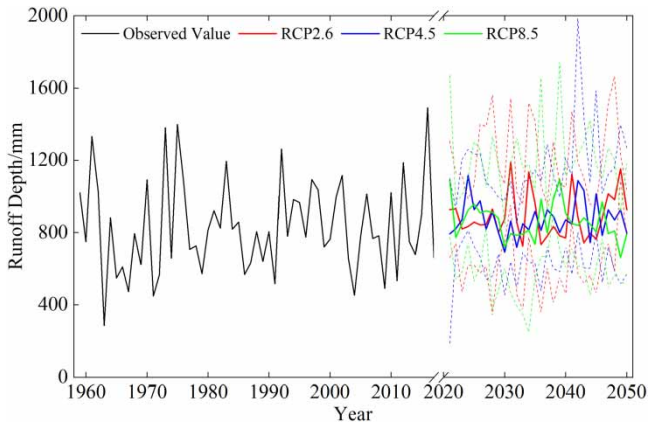

Figure 10 | Annual runoff depth in the study area from 1959 to 2050.

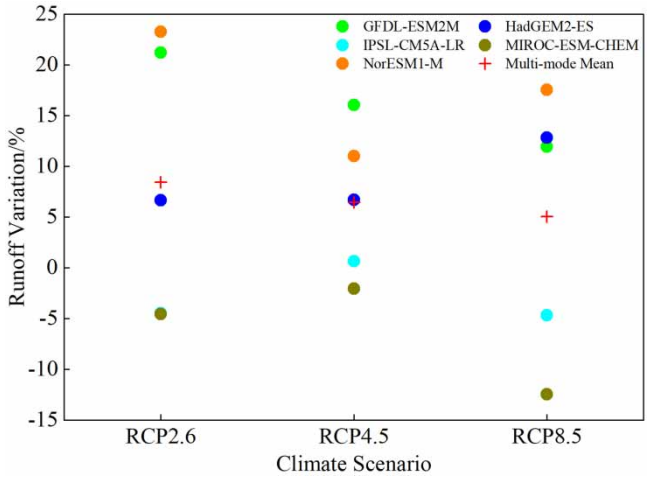

Figure 11 | Runoff variation under various climate scenarios.

evaporation increases; however, in terms of annual runoff, the opposite conclusions are drawn. In this paper, the annual mean runoff is expected to increase by 8.4, 6.5 and 5.0% under three RCPs in the next 30 years, while the latter reported a decreasing trend about −9.9, −19.5 and −11.4%. The reason for the opposite conclusions of projected runoff lies in the different climate models selected. Taking climate models as an example, multiple global GCMs from different countries were selected in this paper, while the latter just chose a climate model, namely BCC CSM1.1. Zhao *et al.* (2020) applied the HBV model and the same five climate models into the GRB to reveal that annual runoff showed an upward trend under the RCP4.5 scenario, while that may decrease after the middle of the 21st century under RCP2.6 and RCP8.5 scenarios. It is evident that the selected hydrological model, study area and study period all have a great influence on the projected runoff.

Since daily-series data of climatic factors are generated by multiple GCMs, the rationality of the results obtained is directly related to the selected climate models, which will create uncertainties inevitably. If different climate models are adopted, the different analyses and conclusions may be achieved in practice. Thus, it is still a challenge to quantitatively describe the variation trend and range for climatic variables.

4. CONCLUSIONS

In this study, precipitation, temperature and runoff in the UGRB were projected, and the impact of climate change on water resources was evaluated by employing the Budyko-type functions driven by multiple representative GCMs. The conclusions are summarized as follows:

- The constructed water-balance model performed well on simulating annual runoff, because *NSE* and *DC* are both >0.84 and >0.64 during two periods. The Budyko-CY function was the optimal water-balance equation screened from the Budyko-Fu, Budyko-Zhang, Budyko-WT and Budyko-CY functions, for its having the maximum *NSE*. Compared with the hydrological model, Budyko-type functions have the advantage of few parameters and simple calculations. Therefore, this approach is appropriate in predicting future streamflow in large-scale regions or ungauged catchments with limited hydrological information.
- When temperature rises by 1 °C, the surface runoff depth is expected to decline by 2.5–4.7% on average, that is 22.6–42.5 mm; when precipitation rises by 10%, surface runoff is expected to rise by 12.1–14.3% on average, that is, 110.7–130.6 mm. The rainfall elasticity of streamflow is strongly correlated to the runoff coefficient, annual rainfall and streamflow, where the runoff coefficient in the UGRB is 0.53, suggesting that this catchment is not sensitive to a climate change.
- The projected temperature over the UGRB presents an obvious escalating trend during the period 2021–2050 with a slope of 0.29 °C/10a, 0.25 °C/10a and 0.61 °C/10a under three RCP scenarios, respectively. The annual mean temperature is estimated to rise by 0.17–1.43, 0.22–1.18 and 0.53–1.72 °C, while the annual runoff is expected to increase slightly with the variability of 8.4, 6.5 and 5.0%, respectively. Five GCMs all show a rise in temperature, with variation ranges of 0.22–0.53 °C (GFDL-ESM2M), 0.92–1.23 °C (HadGEM2-ES), 0.64–1.03 °C (IPSL-CM5A-LR), 1.18–1.72 °C (MIROC-ESM-CHEM) and 0.17–0.64 °C (NorESM1-M), respectively.

As a whole, this research provides possibilities for climate scenarios that may occur in the future and results presented herein are capable of giving a reference to rational allocation and optimal scheduling of water resources in the UGRB. In addition, leveraging of the characteristics of a variety of climate models to prospect surface runoff will remain a tough task over the coming decades.

ACKNOWLEDGEMENTS

This research was financially supported by the Young Elite Scientists Sponsorship Program by CAST (2019QNRC001) and the National Key Research and Development Program of China (2018YFC0407405). The anonymous reviewers and the editor are thanked for providing insightful and detailed reviews that greatly improved the manuscript.

AUTHOR CONTRIBUTIONS

P.S., C.W. and G.D. conducted the research and wrote the paper. J.S., L.K. and M.L. helped to revise the paper. X.L. and H.W. gave the comments. All authors have read and agreed to the published version of the manuscript.

CONFLICTS OF INTEREST

The authors declare no conflict of interest.

DATA AVAILABILITY STATEMENT

All relevant data are included in the paper or its Supplementary Information.

REFERENCES

Bao, Z., Zhang, J., Liu, J., Wang, G., Yan, X., Wang, X. & Zhang, L. 2012 Sensitivity of hydrological variables to climate change in the Haihe River Basin, China. *Hydrological Processes* **26** (15), 2294–2306. doi:10.1002/hyp.8348.

Chen, H., Xu, C. & Guo, S. 2012 Comparison and evaluation of multiple GCMs, statistical downscaling and hydrological models in the study of climate change impacts on runoff. *Journal of Hydrology* **434–435**, 36–45. doi:10.1016/j.jhydrol.2012.02.040.

Chen, Z., Lei, H., Yang, H., Yang, D. & Cao, Y. 2017 Historical and future trends in wetting and drying in 291 catchments across China. *Hydrology and Earth System Sciences* **21** (4), 2233–2248. doi:10.5194/hess-21-2233-2017.

Chiew, F. H. S. 2010 Lumped conceptual rainfall-runoff models and simple water balance methods: overview and applications in ungauged and data limited regions. *Geography Compass* **4** (3), 206–225. doi:10.1111/j.1749-8198.2009.00318.x.

Crow, W. T. & Ryu, D. 2009 A new data assimilation approach for improving runoff prediction using remotely-sensed soil moisture retrievals. *Hydrology and Earth System Sciences* **13** (1), 1–16. doi:10.5194/hess-13-1-2009.

Deng, C. & Wang, W. 2019 Runoff predicting and variation analysis in upper Ganjiang Basin under projected climate changes. *Sustainability* **11** (21), 5885. doi:10.3390/su11215885.

Fang, J., Yu, G., Liu, L., Hu, S. & Chapin, F. S. 2018 Climate change, human impacts, and carbon sequestration in China. *Proceedings of the National Academy of Sciences* **115** (16), 4015–4020. doi:10.1073/pnas.1700304115.

Fu, G., Charles, S. P. & Chiew, F. H. S. 2007 A two-parameter climate elasticity of streamflow index to assess climate change effects on annual streamflow. *Water Resources Research* **43** (11), W11419. doi:10.1029/2007WR005890.

Guan, X., Zhang, J., Bao, Z., Liu, C., Jin, J. & Wang, G. 2021 Past variations and future projection of runoff in typical basins in 10 water zones, China. *Science of The Total Environment* **798**, 149277. doi:10.1016/j.scitotenv.2021.149277.

Jin, J., Wang, G., Zhang, J., Yang, Q., Liu, C., Liu, Y., Bao, Z. & He, R. 2020 Impacts of climate change on hydrology in the Yellow River source region, China. *Journal of Water and Climate Change* **11** (3), 916–930. doi:10.2166/wcc.2018.085.

John, A., Nathan, R., Horne, A., Stewardson, M. & Webb, J. A. 2020 How to incorporate climate change into modelling environmental water outcomes: a review. *Journal of Water and Climate Change* **11** (2), 327–340. doi:10.2166/wcc.2020.263.

Kazemi, H., Sarukkalige, R. & Badrzadeh, H. 2019 Evaluation of streamflow changes due to climate variation and human activities using the Budyko approach. *Environmental Earth Sciences* **78** (24), 1–17. doi:10.1007/s12665-019-8735-9.

Li, D., Pan, M., Cong, Z., Zhang, L. & Wood, E. 2013 Vegetation control on water and energy balance within the Budyko framework. *Water Resources Research* **49** (2), 969–976. doi:10.1002/wrcr.20107.

Li, Z., Li, Q., Wang, J., Feng, Y. & Shao, Q. 2020 Impacts of projected climate change on runoff in upper reach of Heihe River basin using climate elasticity method and GCMs. *Science of the Total Environment* **716**, 137072. doi:10.1016/j.scitotenv.2020.137072.

Liu, Y., Feng, J. & Ma, Z. 2014 An analysis of historical and future temperature fluctuations over China based on CMIP5 simulations. *Advances in Atmospheric Sciences* **31** (2), 457–467. doi:10.1007/s00376-013-3093-0.

Liu, J., Zhang, Q., Singh, V. P. & Shi, P. 2017 Contribution of multiple climatic variables and human activities to streamflow changes across China. *Journal of Hydrology* **545**, 145–162. doi:10.1016/j.jhydrol.2016.12.016.

Piani, C., Weedon, G. P., Best, M., Gomes, S. M., Viterbo, P., Hagemann, S. & Haerter, J. O. 2010 Statistical bias correction of global simulated daily precipitation and temperature for the application of hydrological models. *Journal of Hydrology* **395** (3), 199–215. doi:10.1016/j.jhydrol.2010.10.024.

Piao, S., Ciais, P., Huang, Y., Shen, Z., Peng, S., Li, J., Zhou, L., Liu, H., Ma, Y., Ding, Y., Friedlingstein, P., Liu, C., Tan, K., Yu, Y., Zhang, T. & Fang, J. 2010 The impacts of climate change on water resources and agriculture in China. *Nature* **467** (7311), 43–51. doi:10.1038/nature09364.

Song, P., Liu, W., Sun, J., Wang, C., Kong, L., Nong, Z., Lei, X. & Wang, H. 2020 Annual runoff forecasting based on multi-model information fusion and residual error correction in the Ganjiang River Basin. *Water* **12** (8), 2086. doi:10.3390/w12082086.

Sun, G. & Peng, F. 2020 Evaluation of future runoff variations in the north–south transect of eastern China: effects of CMIP5 models outputs uncertainty. *Journal of Water and Climate Change* **11** (4), 1355–1369. doi:10.2166/wcc.2019.261.

Taylor, K. E., Stouffer, R. J. & Meehl, G. A. 2012 An overview of CMIP5 and the experiment design. *Bulletin of the American Meteorological Society* **93** (4), 485–498. doi:10.1175/BAMS-D-11-00094.1.

Teng, J., Chiew, F. H. S., Vaze, J., Marvanek, S. & Kirono, D. G. C. 2012 Estimation of climate change impact on mean annual runoff across continental Australia using Budyko and Fu equations and hydrological models. *Journal of Hydrometeorology* **13** (3), 1094–1106. doi:10.1175/JHM-D-11-097.1.

Thompson, J. R., Green, A. J., Kingston, D. G. & Gosling, S. N. 2013 Assessment of uncertainty in river flow projections for the Mekong River using multiple GCMs and hydrological models. *Journal of Hydrology* **486**, 1–30. doi:10.1016/j.jhydrol.2013.01.029.

Wang, D. & Tang, Y. 2014 A one-parameter Budyko model for water balance captures emergent behavior in Darwinian hydrologic models. *Geophysical Research Letters* **41** (13), 4569–4577. doi:10.1002/2014GL060509.

Warszawski, L., Frieler, K., Huber, V., Piontek, F., Serdeczny, O. & Schewe, J. 2014 The inter-sectoral impact model intercomparison project (ISI–MIP): project framework. *Proceedings of the National Academy of Sciences* **111** (9), 3228–3232. doi:10.1073/pnas.1312330110.

Wen, X., Fang, G., Qi, H., Zhou, L. & Gao, Y. 2016 Changes of temperature and precipitation extremes in China: past and future. *Theoretical and Applied Climatology* **126** (1), 369–383. doi:10.1007/s00704-015-1584-x.

Wu, J. & Miao, C. 2017 Contribution analysis of the long-term changes in seasonal runoff on the Loess Plateau, China, using eight Budyko-based methods. *Journal of Hydrology* **545**, 263–275. doi:10.1016/j.jhydrol.2016.12.050.

Wu, J., Miao, C., Zhang, X., Yang, T. & Duan, Q. 2017 Detecting the quantitative hydrological response to changes in climate and human activities. *Science of the Total Environment* **586**, 328–337. doi:10.1016/j.scitotenv.2017.02.010.

Xing, W., Wang, W., Zou, S. & Deng, C. 2018 Projection of future runoff change using climate elasticity method derived from Budyko framework in major basins across China. *Global and Planetary Change* **162**, 120–135. doi:10.1016/j.gloplacha.2018.01.006.

Yan, Z., Zhou, Z., Liu, J., Han, Z., Gao, G. & Jiang, X. 2020 Ensemble projection of runoff in a large-scale basin: modeling with a global BMA approach. *Water Resources Research* **56** (7), e2019WR026134. doi:10.1029/2019WR026134.

Yu, Z., Tan, G. & Li, G. 2014 Characteristic analysis of inflow and water resources in the Poyang Lake Basin. *Journal of Water Resources Research* **3**, 465–472 (in Chinese).

Yuan, F., Tung, Y. & Ren, L. 2016 Projection of future streamflow changes of the Pearl River basin in China using two delta-change methods. *Hydrology Research* **47** (1), 217. doi:10.2166/nh.2015.159.

Yuan, Z., Yan, D., Yang, Z., Yin, J., Zhang, C. & Yuan, Y. 2017 Projection of surface water resources in the context of climate change in typical regions of China. *Hydrological Sciences Journal* **62** (2), 283–293. doi:10.1080/02626667.2016.1222531.

Yuan, Z., Xu, J. & Wang, Y. 2018a Projection of future extreme precipitation and flood changes of the Jinsha River Basin in China based on CMIP5 climate models. *International Journal of Environmental Research and Public Health* **15** (11), 2491. doi:10.3390/ijerph15112491.

Yuan, Z., Yan, D., Yang, Z., Xu, J., Huo, J., Zhou, Y. & Zhang, C. 2018b Attribution assessment and projection of natural runoff change in the Yellow River Basin of China. *Mitigation and Adaptation Strategies for Global Change* **23** (1), 27–49. doi:10.1007/s11027-016-9727-7.

Yuan, Z., Xu, J., Wang, Y., Hong, X., Zhou, Y. & Chen, J. 2019 Long-term projection of surface runoff in the Fu River basin based on water-energy balance. *Advanced Engineering Sciences* **51** (1), 60–67 (in Chinese).

Zhang, P., Lei, X., Wang, X. & Wang, C. 2018a Optimal water regulation in middle and lower reaches of Ganjiang River based on water demand control strategy. *Yangtze River* **49** (12), 43–48 + 86 (in Chinese).

Zhang, S., Yang, Y., McVicar, T. R. & Yang, D. 2018b An analytical solution for the impact of vegetation changes on hydrological partitioning within the Budyko framework. *Water Resources Research* **54** (1), 519–537. doi:10.1002/2017WR022028.

Zhao, M., Su, B., Wang, Y., Wang, A. & Jiang, T. 2020 Impacts of climate change on river runoff at the Ganjiang and Guanting River basins in the eastern monsoon region. *Climate Change Research* **16** (6), 679–689 (in Chinese).

Zhou, T., Wang, B., Yu, Y., Liu, Y., Zheng, W., Li, L., Wu, B., Lin, P., Guo, Z., Man, W., Bao, Q., Duan, A., Liu, H., Chen, X., He, B., Li, J., Zou, L., Wang, X., Zhang, L., Sun, Y. & Zhang, W. 2018 The FGOALS climate system model as a modeling tool for supporting climate sciences: an overview. *Earth and Planetary Physics* **2** (4), 276–291. doi:10.26464/epp2018026.

Zhu, X., Zhang, A., Wu, P., Qi, W., Fu, G., Yue, G. & Liu, X. 2019 Uncertainty impacts of climate change and downscaling methods on future runoff projections in the Biliu River Basin. *Water* **11** (10), 2130. doi:10.3390/w11102130.

Zinyengere, N., Theodory, T. F., Gebreyes, M. & Speranza, C. I. 2017 *Beyond Agricultural Impacts: Multiple Perspectives on Climate Change and Agriculture in Africa*. Academic Press, London, UK.

First received 2 July 2021; accepted in revised form 30 December 2021. Available online 24 January 2022